Fracture of alpha titanium alloys at high strain rates and stress triaxiality

†VladimirV. Skripnyak[1], Alexander A. Kozulyn[1], Evgeniya G. Skripnyak[1], and VladimirA. Skripnyak[1]

[1]Research Laboratory of Properties of Substances in Extreme States, National Research Tomsk State University, Russia

*Presenting author: skrp2012@yandex.ru
†Corresponding author: skrp2012@yandex.ru

Abstract

The aim of this work was the evaluation of combined effect of stress triaxiality and strain rate on the mechanical behavior of the alpha titanium alloys. Mechanical behaviour of titanium alloy Grade 6 (VT5-1 or Ti-5Al-22,5Sn) and Grade 2 (VT1-0) in a range of strain rates from 0.001 to 1000 1/s and stress triaxiality (0.3–0.6) at room temperature was studied using an Instron VHS 40 / 50-20 servo-hydraulic test machine. Analysis of stress state and strain distribution in smooth and notched samples under tension was carried out by means of computer simulation and analytical relations. The Gurson-Tvergaard-Needleman model, complemented with phenomenological laws for voids nucleation, growth and coalescence, was adopted for describing the fracture of the alpha titanium alloys. It was shown that stress triaxiality is important for prediction of damage evolution and fracture of alpha titanium alloys at high strain rates. The constitutive equation and fracture models have been validated by simulating the tension tests. It was obtained that strain localization phenomena play a major role in the fracture process at lower triaxiality. It is found that the strain to fracture of alpha titanium alloy is strongly depended on the stress triaxiality and strain rate above 100 s^{-1}. The strain to failure of alpha titanium alloys at room temperature decrease by 3.7 times with increasing stress triaxiality from 0.3 to 0.6 in wide range of strain rates.

Keywords: **Computer simulation, mechanical behavior, ductility, titanium alloys, high strain rate, stress triaxiality**

Introduction

Polycrystalline alpha-titanium alloys belong to the isomechanical group of metal materials with hexagonal close packed (HCP) crystalline lattice. Materials belonging to the same mechanical group possess similarity of mechanical behavior in wide ranges of strain rates and temperature owing to similarity of mechanisms of plastic deformation and fracture. [1].

Generalization of data on the laws of deformation and fracture of alpha titanium alloys in a wide range of strain rates will allow developing a method for prediction of titanium structural elements under dynamic impacts [2]-[5]. It was shown that the ductility and strength of titanium alloys in a wide range of strain rates depends on the grain size and a grain size distribution [5]-[9]. There is evidence that the ductility and fracture of the hexagonal close packed polycrystalline metals and alloys is strongly dependent on the accumulated plastic strain and stress triaxiality [10[-[13]. The dimensionless stress triaxiality η, defined as the ratio between the hydrostatic stress and equivalent stress [10][11][14].

A significant distinction has been noted between the regimes of high and low stress triaxiality. High values of triaxiality (i.e., $\eta > 1.5$) may be achieved in local areas, such as at the ends of the cracks or in the center of a necking or notched specimen under tension. Low stress triaxiality takes place at surfaces and protruding corners, where the equivalent shear stress is high relative to the hydrostatic pressure [15]-[19]. At low stress triaxiality the fracture initiation is strongly inhibited.

Several models were proposed for investigation of the effect of triaxiality on the fracture of polycrystalline metals and alloys [20]-[24]. Neilsen and Tvergaard [20][21] showed that ductile fracture can be described using the criterion, depending on the stress triaxiality and the Lode angle. Valoppi and others [11] used the phenomenological Johnson Cook hardening model and damage initiation criterion with an energy-based law describing the damage evolution in the finite element models for titanium alloy. It was shown, the Gurson–Tvergaard–Needleman plasticity model can be complemented with phenomenological laws for void nucleation, growth and coalescence [10][21]. In this research we study the influence of different values of stress triaxiality ($0.33< \eta < 0.6$) on ductile fracture in a wide range of strain rates using experimental tests and numerical simulation. Four types of VT 5-1 (Ti-5Al-22,5Sn) sheet samples were used in experiments on static and dynamic tension.

1 Material and samples

Sheets of alpha titanium alloys VT 5-1 (Grade 6) and VT1-0 (Grade 2) were studied under tension in a range of strain rates from 0.01 to 1000 s^{-1} at room temperature. The thickness of the sheet samples VT5-1 and VT1-0 was 1.15±0.05 mm, and 1.1±0.05 mm, respectively. Samples of alloys VT5-1 and VT1-0 had an average grain size of 40 μm and 30 μm, respectively. Samples characterized by different geometries were used for tensile test, as shown in Fig. 1(a).

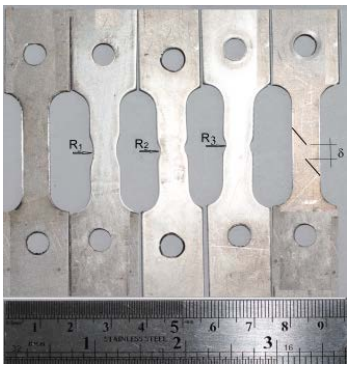

Figure 1. Geometry of the samples used for the tensile and shear tests

The samples were cut using electro erosion cutting method from a sheet of titanium alloy. The initial gauge length l_0 was equal to 24±0.1 mm. The cross-sectional area of the smooth flat samples was A_0=9.3±0.05 mm2, and notch flat specimens had notch radiuses of R_1=10 mm, R_2 = 5 mm, R_3=2 mm, respectively. The samples for shear test had distance between cuts δ ~4.5 mm.

The stress triaxiality η and Lode parameter L defined as [25]:

$$\eta = -p/\sigma_{eq},\ L = (2\sigma_{II} - \sigma_I - \sigma_{III})/(\sigma_I - \sigma_{III}), \quad (1)$$

where p is the pressure, σ_I, σ_{II}, σ_{III} are first, second, and third invariants of the Cauchy stress tensor respectively, $\sigma_{eq} = (3\sigma_{II})^{1/2}$ is the equivalent stress.
The initial value of the stress triaxiality η calculated by the analytical formula in the plane stress state [14]:

$$\eta = (1+2D)/(3\sqrt{D^2+D+1}),\ D = \ln[1+a/(4R)], \quad (2)$$

where a is the width of sample, R is the value of curvature radius.
The initial value of the stress triaxiality has varied in the range 0.0–0.6 in experiments.

The stress triaxiality η will be slightly different from the initial value when the sample neck is formed.

2 Quasistatic and dynamic tests

The tests were carried out in a range of strain rates ($0.001-1000\ s^{-1}$) at room temperature using the Instron test machine VHS 40/50-20 with a 50 kN load cell.
The tensile force and displacement of the specimen were recorded at high temporal resolution up to complete fracture of the specimen. The constant tension velocities (20±0.01, 12±0.01, 2.4±0.002, 0.4±0.001 m/s) were supported during tests.
Tests were divided into three groups. First group is uniaxial tensile tests carried out on smooth specimens, characterized by positive values of both the stress triaxiality and Lode parameter. The second group is pure shear tests. The third group is uniaxial tensile tests carried out on notched specimens. Three values of notch radius, 2 mm, 5 mm and 10 mm, were used in this study.

True strain and true stress at time moments of loading were determined by analytical relations [11]:

$$\varepsilon_1^{true} = \ln(1+\Delta l / l_0),\ \sigma_1^{true} = (F / A_0)(1+\Delta l / l_0), \quad (3)$$

where ε_1^{true} is true strain, σ_1^{true} is true stress, F is tensile force, A_0 is mean initial minimum cross sectional area of sheet sample, Δl, *and* l_0 are the elongation and the initial length of sample working part.

True stresses and true strains were also determined by computer simulation of the specimen deformation process. The results of numerical simulation were used in which a good agreement was reached between the calculated and experimental values of the sample forces and displacements versus time.

3 Computational model

The computational model uses the theoretical basis of continuum damage mechanics [26]. Mechanical behaviour was described by a system of conservation equations (mass, momentum and energy), kinematic equation and the constitutive equation. Initial and boundary conditions were added to the system of equations. The boundary conditions correspond to the conditions of loading of the 3D body. Dog bone specimens were simulated under axial tension with a constant strain rate. The computer simulations were performed with the use of licensed LS DYNA software, and being a part of the package simulation of the dynamic loads of the package ANSYS WB 15.2. The calculations were carried out using solvers using finite-difference scheme of second order accuracy. The grid model of the samples used in tests is shown in Fig. 2.

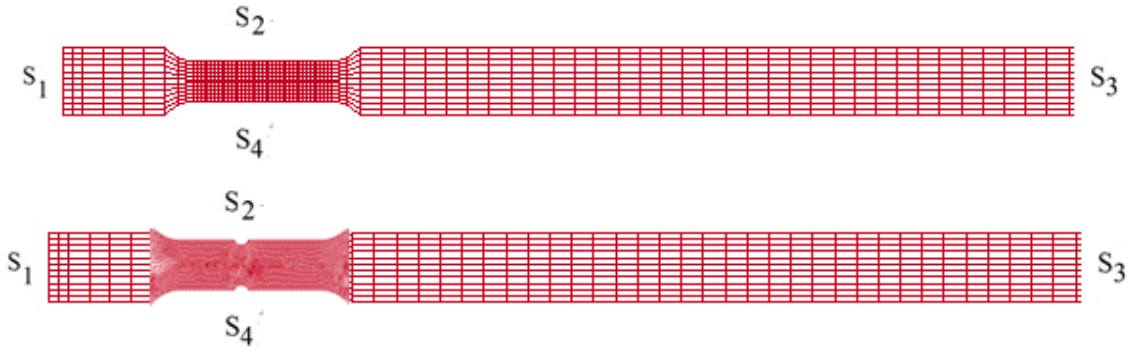

Figure 2. Grid models of flat samples

Boundary conditions corresponding to uniaxial tension of the sample at a constant strain rate have the form:

$$\begin{aligned} u_x|_{S_1} &= 0, \quad u_x|_{S_3} = 0, \\ u_y|_{S_1} &= 0, \quad u_y|_{S_3} = v_{y_0}, \\ u_z|_{S_1} &= 0, \quad u_z|_{S_3} = 0, \\ \sigma_{ij}|_{S_2 \cup S_4 \cup S_5 \cup S_6} &= 0, \end{aligned} \tag{4}$$

where $u_i|_{S_j}$ is the components of the particle velocity vector on the surface S_j, v_{y_0} is the tensile velocity, σ_{ij} is the components of the stress tensor.

The initial conditions correspond to the free stress state of the material in a uniform temperature field.

The flow stress of alloys has been described using a modification of the Johnson-Cook model (5) and the Zerilli–Armstrong model (6) [2] [11][27]

$$\sigma_s = \{A + B(\varepsilon_{eq}^P)^n + kd_g^{-1/2}\}[1 + C\ln(\dot{\varepsilon}_{eq}/\dot{\varepsilon}_{eq0})]\{1 - [\frac{T - T_0}{T_m - T_0}]^m\}, \tag{5}$$

where A, B, C, n, m, k are constants of material, d_g is the grain size, $\dot{\varepsilon}_{eq} = [(2/3)\dot{\varepsilon}_{ij}\dot{\varepsilon}_{ij}]^{1/2}$, $\dot{\varepsilon}_0 = 1.0\,s^{-1}$, $\varepsilon_{eq}^P = \int_0^t [(2/3)\dot{\varepsilon}_{ij}^P \dot{\varepsilon}_{ij}^P]^{1/2} dt$ is the plastic strain intensity, T is the temperature, T_0 is the room temperature, and T_m is the melting temperature.

Material constants of the equation (13) of alpha titanium alloys are given in Table 1.

Table 1. Material constants of modified Johnson-Cook model

Coefficient / Titanium alloy	A, GPa	B, GPa	n	k_g, GPa $nm^{1/2}$	C	m at $T \le T_\beta$	T_m, K
VT1-0	0,244	0,86	0,475	6,2	0,027	0.7	1946
VT5-1	0,760	0,86	0,5	6,2	0,027	0.64	1888

T_β is equal to 1313K and 1183 for VT5-1 and VT1-0, respectively.

Updating of the constitutive equation of the Armstrong - Zerilli model can be written in the following form [27]:

$$\sigma_s = \sigma_{s0} + C_5(\varepsilon_{eq}^p)^{n_1} + k_{hp}d_g^{-1/2} + C_2\exp\{-C_3T + C_4T\ln(\dot{\varepsilon}_{eq}/\dot{\varepsilon}_{eq0})\}. \tag{6}$$

Material parameter σ_{s0}, C_5, n_1, k_{hp}, C_2, C_3, C_4 of alpha titanium alloys are given in Table 2.

Table 2. Material parameter of the Armstrong-Zerilli model

Coefficient / Titanium alloy	σ_{s0}, GPa	k_{hp}, GPa $nm^{1/2}$	C_2, GPa	C_3, K^{-1}	C_4, K^{-1}	C_5, GPa	n_1
VT1-0 (Grade 2)	0,138	6,2	0,1843	0,000877	0,0004	0.62	0.5
VT5-1 (Grade 6)	0,41	6,2	0,1843	0,000877	0,0004	1.84	0.5

Fig. 3 shows the calculated yield stress and experimental true stress versus true strain curves.

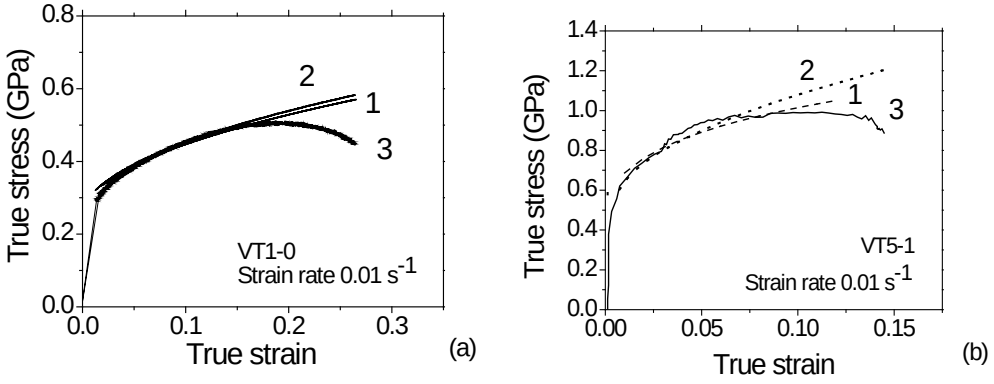

Figure 3. Calculated stress versus strain and experimental true stress vs true strain curves of (a) VT1-0 and (b) VT5-1; Johnson-Cook (curves 1) and modified Zerilli-Armstrong model prediction (curve 2)

Curves 1 were calculated by Johnson-Cook constitutive equation (5) and curves 2 by modified Zerilli-Armstrong equation (6). Curves 3 are experimental data on VT1-0 (Fig3(a)) and VT5-1 titanium alloys (Fig 3(b)). Grain size was assumed ~30 μm for VT1-0 and 40 μm for VT5-1. Experimental and calculated yield stresses correspond to strain rate of 0.01 s^{-1}.

4 Damage model

Ductile fracture is considered as a result of void nucleation, growth and coalescence under a triaxle stress states or shear localization at low stress triaxiality [10]. One of the most widely used damage models for ductile fracture was proposed by Gurson with subsequent development in the works of Tvergaard and Needleman [15][20][21]. This Gurson-Tvergaard-Needleman (GTN) model [20][21] was used for analysis of stresses and strains in smooth and notched samples of sheet VT 5-1 under tension. The yield criterion has a form:

$$(\sigma_{eq}{}^2 / \sigma_s{}^2) + 2q_1 f^* \cosh(-q_2\, p / 2\sigma_s) - 1 - q_3 (f^*)^2 = 0, \qquad (7)$$

where σ_s is the yield stress, p is the pressure, q_1, q_2 and q_3 are model parameters, f is the void volume fraction.

The rate of void growth is obtained by assuming mass conservation and depends on the volume change part of the plastic strain.
Consequently, there is no void growth in pure shear deformation. The void nucleation depends on the equivalent plastic strain ε_p, here a normal distribution A is used.
A strong coupling between deformation and damage is introduced by a plastic potential function which is dependent on the void volume fraction f*:

$$\begin{aligned} \dot{f} &= \dot{f}_{nucl} + \dot{f}_{growth}, \\ \dot{f}_{nucl} &= (f_N / s_N)\dot{\varepsilon}^p \exp\{-0.5[\varepsilon^p{}_{eq} - \varepsilon_N) / s_N]^2\}, \\ \dot{f}_{growth} &= (1-f)\dot{\varepsilon}^p_{kk}, \end{aligned} \qquad (8)$$

where ε_N and s_N are the average nucleation strain and the standard deviation respectively. The amount of nucleating voids is controlled by the parameter f_N.

$$f^* = f \text{ if } f \le f_c;$$
$$f^* = f_c + (\bar{f}_F - f_c)/(f_F - f_c) \text{ if } f > f_c, \quad (9)$$

where $\bar{f}_F = (q_1 + \sqrt{q_1^2 - q_3})/q_3$, q_1, q_2, and q_3 are constants of the model.

The final stage in ductile fracture comprises in the voids coalescence into the fracture zone. This causes softening of the material and accelerated growth of the void fraction f* until the fracture void fraction f_F is reached. At this moment the material is fractured.

The model of ductile fracture requires knowledge of 9 parameters: three model parameters (q_1, q_2 and q_3), the initial void fraction f_0, three void nucleation parameters (ε_N, s_N and f_N), two failure parameters (f_c and f_F). The model parameters for titanium alloy VT 5-1 and VT1-0 were determined by numerical simulation of experiments on the tensile samples in the velocity range from 20 to 0.4 m/s. Numerical values of model parameters were fitted

Numerical values of model parameters are given in Table 3. The model was used for simulation samples under tension at constant velocity from 20 m/s to 0.4 m/s.

Table 3. Dimensionless parameters for the GTN model for alpha titanium alloys

Parameter	q_1	q_2	q_3	f_0	f_N	fc	f_F	ε_N	s_N
VT 5-1 (Grade 6)	1	0.7	1	0.00	0.156	0.117	0.26	0.05	0.1
VT1-0 (Grade 2)	1.5	1	2.25	0.002	0.017	0.26	0.303	0.3	0.1

5 Results and discussion

The character of fracture of the samples at tensile velocities of 20 m / s, 12 m / s, 2.4 m / s, and 0.4 m / s can be seen in Fig. 4. The cracks position indicates that there is a very strong correlation between the localization of the plastic deformation and damage growth.

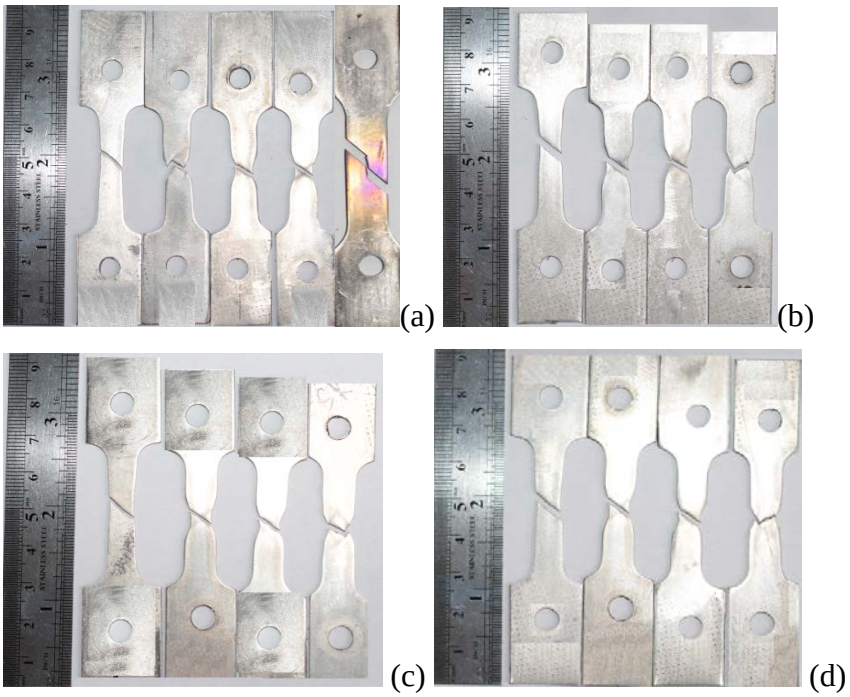

Figure 4. Fractured smooth and notched samples of VT5-1 titanium alloy after tension at the velocity: (a) 20 m/s , (b) 12 m/s, (c) 2.4 m/s, (d) 0.4 m/s

Principal tensile stress, effective stress, effective plastic strain in the notched specimen of an alpha titanium alloy VT5-1 before crack initiation are shown in Fig. 5 (a), (b), (c), respectively. Effective plastic strain near crack is shown in Fig. 5(c, d).

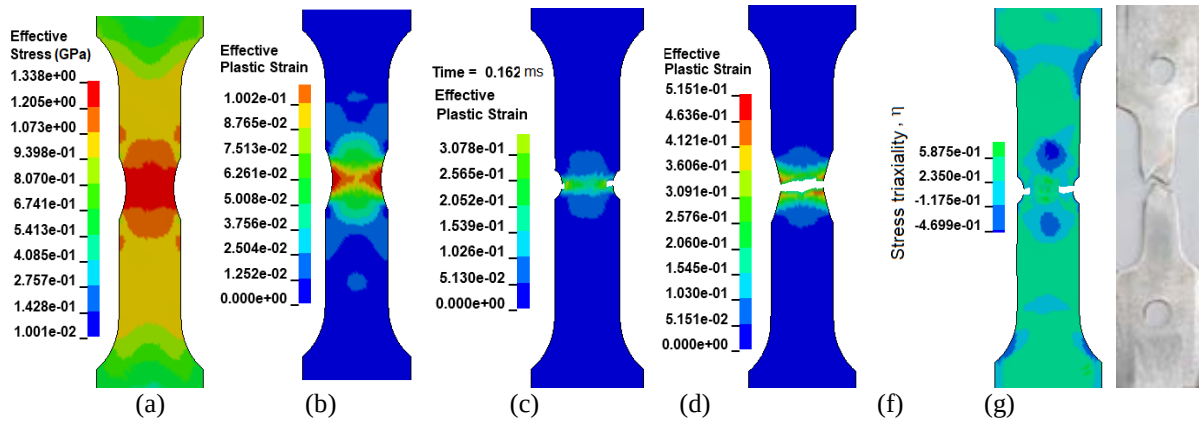

Figure 5. (a) Effective stress, (b), (c), (d) effective plastic strain in the alpha titanium notched specimen under tension at 20 m/s; (f) stress triaxiality; (g) photo of fractured notched specimen

For notched specimens under uniaxial tension damage can initiates at the outer surface of the specimen, and grows from the outer surface to the center of the specimen. The simulations demonstrate the important role of strain localization phenomena in the fracture processes. Figure 6 shows the calculated plastic strain in the necking zone before fracture. Two inclined stationary shear bands were formed in the necking zone. Fig. 5 and 6 showed the calculated configuration of cracks.

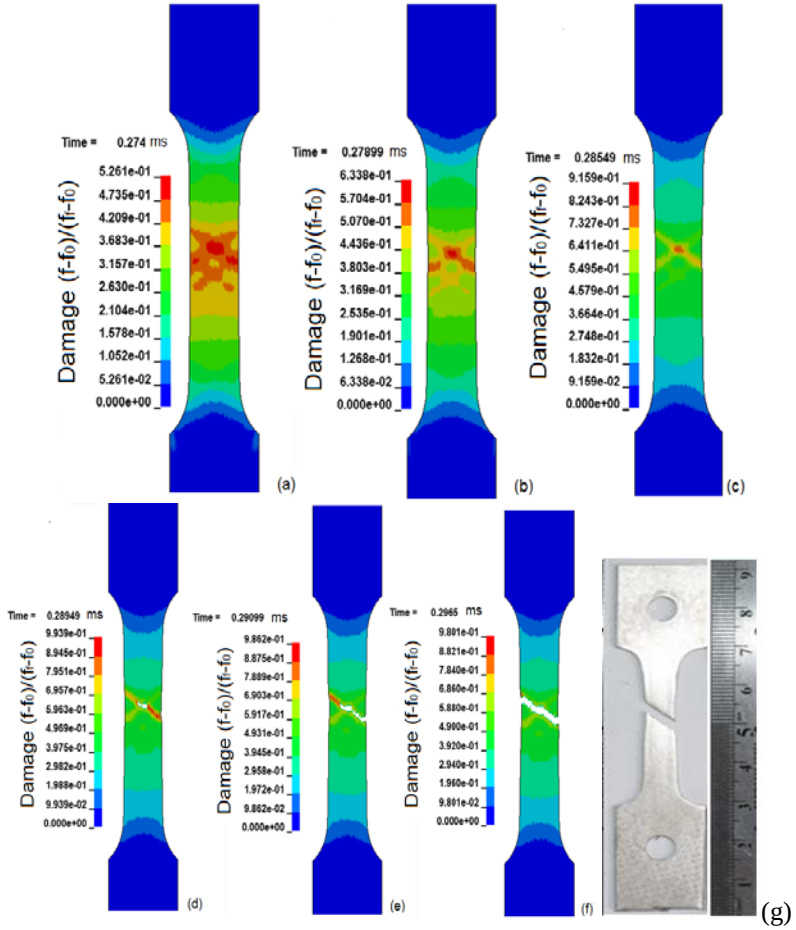

Figure 6. Damage growth and crack initiation in the alpha titanium smooth specimen under tension at 20 m/s; (g) photo of fractured specimen

Calculated configurations have good agreement with experimental data (See Fig.5(a)). Verleysen showed that the phenomena of strain localization play a major role in the fracture process of alpha+beta titanium alloy (Ti6V4Al) at lower stress triaxiality [25]. The experimental and theoretical results obtained in this paper on alpha titanium alloys agree with the results for two-phase alpha + beta titanium alloys. Damage evolution in smooth specimen of alpha titanium alloy (VT5-1) under tension is shown in Fig.6.

The growth of damage and the initiation of cracks in the smooth sample of alpha-titanium under tension at 20 m / s occur in the shear bands. Localized shear bands at the first stages of deformation are non-stationary (See Fig. 6(a,b)) and intersect at angles. Calculated configuration of cracks in the smooth and notched samples of alpha titanium alloys is in good agreement with the experimental data.

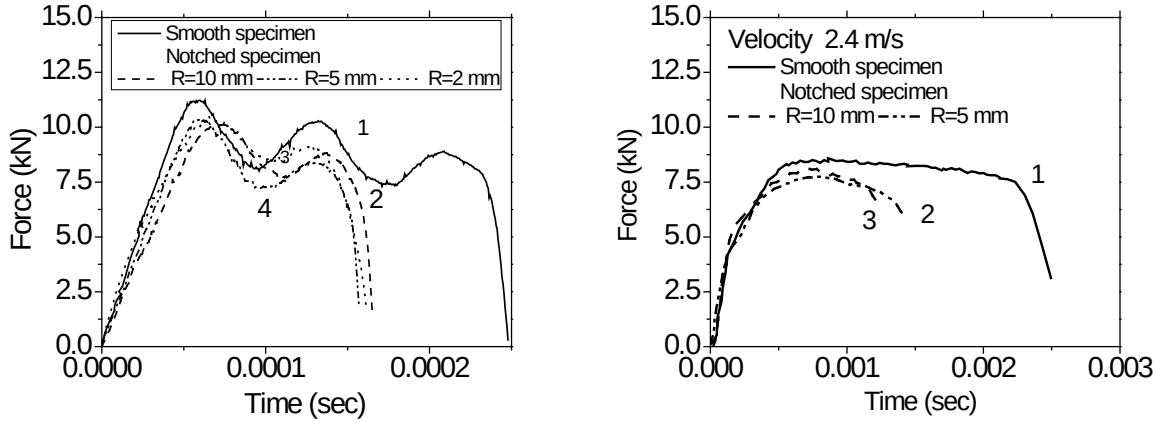

Figure7. Measured force versus time under tension smooth and notch samples (a) at 20.0±0.01 m/s and (b) 2.4 m/s

The force versus time at room temperature and tension velocity of 20 m/s and 2.4 m/s are shown in Fig. 7(a) (b), respectively. The shape of force versus time curves depends on the distance between the grips and the tensile speed.

Using «fast jaw» grips on the Instron test machine VHS 40/50-20 during high-rate tests with different velocities of tension leads to the need to account for changes in the distance between the grips when determining the true stress and true strain curves. Oscillations of the force shown in Fig 7 (a) are caused by the reflection of the force pulses moved through the specimen.

Therefore, the use of the analytical ratio (3) to analyze the results of tests at high tensile velocity leads to the need for averaging the data obtained. The true stress obtained from analytical relations (3) is underestimated relative to the values obtained by numerical simulation. The true stress versus true strain at room temperature and strain rate 834 s^{-1} (at the velocity 20 m/s) are shown in Fig. 8 (a). The introduction of the triaxiality effect in the strain hardening model is important for the prediction of damage evolution under deformation at high strain rates. Damage kinetics in alpha titanium alloys is connected with macroscale plastic instability. Strain to fracture at strain rates 833±5, 418 ±2, 100±1, 16.7±1 s^{-1} of smooth and notched samples are shown in Fig. 8(b). The strain to fracture of the alpha-titanium alloy is reduced simultaneously with the growth of the strain rate from 0.01 to ~1000 s^{-1} and also reduced with an increase in the stress triaxiality η in the range from 0.33 to 0.55.

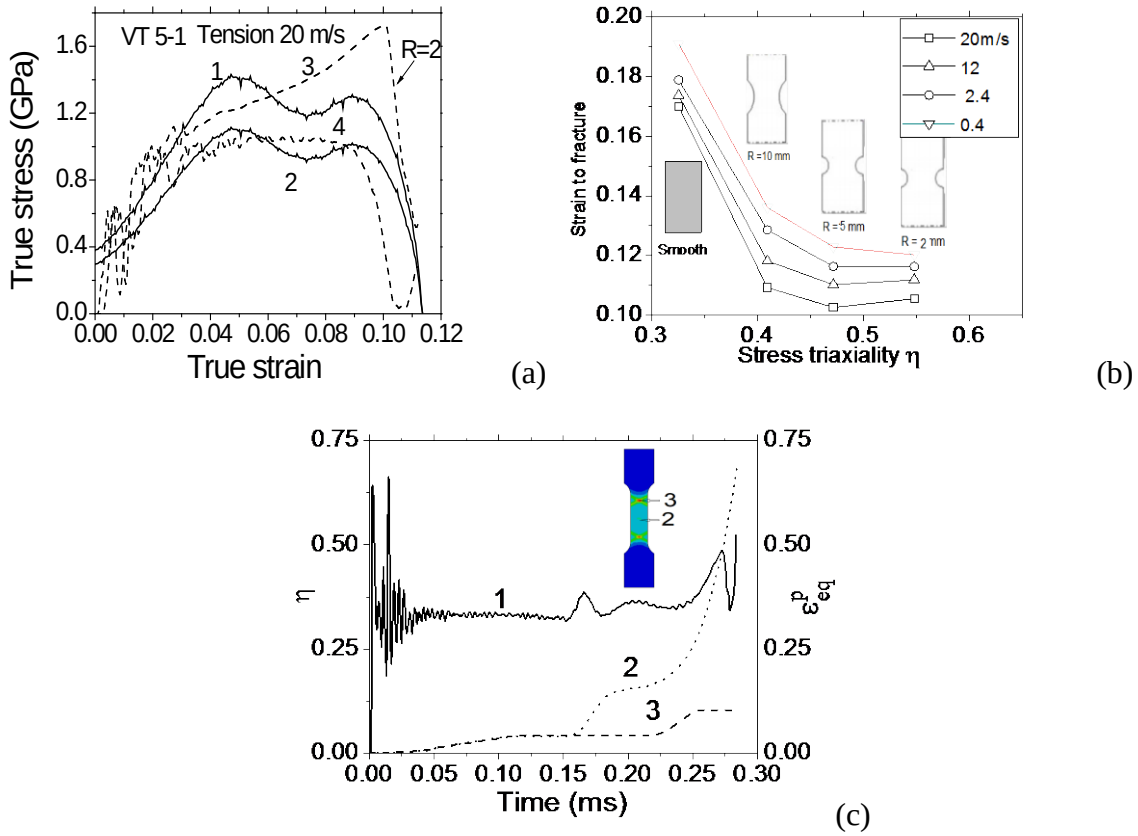

Figure 8. (a) The true stress versus true strain of titanium VT 5-1 at room temperature: analytical curves (1), and (2); calculated curves (3), and (4); (b) strain to fracture samples under uniaxial tension at velocities 20, 12, 2.4, 0.4 m/s and at the initial stress triaxiality η: 0.3333, 0.4087, 0.4681, 0.5491; (c) stress triaxiality in the gauge 2 (curve 1), equivalent plastic strain in gauges 2 and 3 (curves 2,3)

The stress triaxiality at strain rate above 100 s^{-1} is strongly influenced on the plastic flow and fracture of alpha titanium alloy. Strain to failure of alpha titanium alloys at room temperature decrease by 3.7 times with increasing stress triaxiality from 0.3 to 0.6 at strain rates of 0.01-1000 s^{-1}.

The results on the influence of stress triaxiality on the strain to fracture of the alpha titanium alloys obtained in this paper agree with the data of Bobbili [13].

The simulation results showed that stress triaxiality is changed in the necking zone under tension (see Fig.8(c)). The variation of η in the necking zone is caused by the shear stress relaxation at quasi -stationary shear bands formation.

The use of a model combining the description of the plastic flow of origin and the growth of damage in the calculations made it possible to compare the description of the mechanical behavior of alpha-titanium alloys in the strain rate range from 0.001 to 1000 s^{-1} and different values of stress triaxiality (0.0< n < 0.6).

Conclusions

In this paper, mechanical behavior of titanium alloy Grade 6 (this is an analog of VT5-1 or Ti-5Al-22,5Sn) and Grade 2 (VT1-0) was studied under tension in a wide range of strain rates (from 0.001 to 1000 1/s) and stress triaxiality (0.0–0.6) at room temperature. Smooth and notched specimens were tested at tension velocity from 0.04 m / s to 20 m/s using an Instron VHS 40 / 50-20 servo-hydraulic test machine.

Analysis of the experimental results is supported by finite element simulations. Detailed information, complementary to the test results, is obtained on the stress and strain distribution close to the fracture. A ductile fracture at high strain rates occurs in smooth and notched samples.
A coupled elastic-plastic-damage model based on continuum damage theory used to simulate the mechanical behavior of alpha titanium alloys with HCP crystal structure.
The Gurson-Tvergaard-Needleman damage model is adopted for alpha titanium alloys, complemented with phenomenological laws for void nucleation, growth and coalescence.
The model can accurately predict both deformation and damage behaviors of alpha titanium alloys at strain rates from 0.001 to 1000 s-1 and stress triaxiality from 0.3 to 0.6.
The obtained experimental data indicate that there is a very strong correlation between the characteristics of the plastic deformation and the rate of damage growth.
The constitutive and failure model parameters can be determined on the base of tensile test results. The constitutive and fracture models have been validated by simulating the tension tests.

Acknowledgement
This work was supported partially by the Grant from the President of Russian Federation MK-2690.2017.8 and by The Tomsk State University competitiveness improvement programme. The authors are grateful for the support of this research.

References

[1] Frost H.J., Ashby M.F., *Deformation-mechanism maps*. Oxford: Pergamon Press; 1982. 166 p.
[2] Gao C.Y., Zhang L.C., and Yan H.X. (2011) A new constitutive model for HCP metals, *Materials Science and Engineering A* **528**, 4445–4452.
[3] Xu Q., Meyers M.A., and Nesterenko V.F. (2002) Self-organization of shear bands in titanium and Ti–6Al–4V alloy, *Acta Materialia* **50**, 575-596.
[4] Herzig N., Meyer L.W., Musch D., Halle T., Skripnyak V.A., Skripnyak E.G., Razorenov S.V., Krüger L. (2008) The mechanical behaviour of ultrafine grained titanium alloys at high strain rates, *3rd International Conference on High Speed Forming* – March 11-12, 2008. Dortmund, Germany. -14 p. DOI:10.17877/DE290R-8660
[5] Skripnyak V. A. and Skripnyak E. G. *Mechanical behaviour of nanostructured and ultrafine-grained metal alloy under intensive dynamic loading*, Chapter 2: *Nanotechnology and Nanomaterials» "Nanomechanics"*, Eds.by A. Vakhrushev, ISBN 978-953-51-3182-3, Print ISBN 978-953-51-3181-6, 2017. DOI: 10.5772/Intech open.68291.
[6] Skripnyak V.A., Skripnyak N.V., Skripnyak E.G., Skripnyak V.V. (2017) Influence of grain size distribution on the mechanical behavior of light alloys in wide range of strain rates, *AIP Conference Proceedings*, 1793, art. no. 110001.
[7] Skripnyak N.V., Skripnyak E.G., Skripnyak V.A., Skripnyak V.V., Vaganova I.K. (2014) Failure mechanisms of light alloys with a bimodal grain size distribution *11th World Congress on Computational Mechanics, WCCM 2014, 5th European Conference on Computational Mechanics, ECCM 2014 and 6th European Conference on Computational Fluid Dynamics, ECFD*, 3915-392.
[8] Sharkeev Y.P., Vavilov V.P., Belyavskaya O.A., Skripnyak V.A., Nesteruk D.A., Kozulin A.A., Kim V.M. (2016) Analyzing deformation and damage of VT1-0 titanium in different structural states by using infrared thermography, *Journal of Nondestructive Evaluation,* 35 (3), Art. no. 42.

[9] Ratochka I.V., Lykova O.N., Geraskina A.Yu. and Skripnyak V.A. (2009) Grain boundary sliding in a submicrocrystalline Ti–6Al–4V titanium alloy under superplastic deformation, *Fiz. Mezomekh* **12**, No. 5, 97-101.
[10] Y. Bai and T. Wierzbicki, A new model of metal plasticity and fracture with pressure and Lode dependence, *International Journal of Plasticity* **24**, 1071–1096, 2008.
[11] Valoppi B., Bruschi S., Ghiotti A., Shivpur R. (2017) Johnson-Cook based criterion incorporating stress triaxiality and deviatoric effect for predicting elevated temperature ductility of titanium alloy sheets, *International Journal of Mechanical Sciences* **123**, 94-105.
[12] Revil-Baudard B., Cazacu O., Flater P., Chandola N., and Alves J.L. (2016) Unusual plastic deformation and damage features in titanium: Experimental tests and constitutive modeling, *Journal of the Mechanics and Physics of Solids* **88**, 100-122.
[13] Bobbili R., and Madhun V. (2016) Flow and fracture characteristics of near alpha titanium alloy, *Journal of Alloys and Compounds* **684**, 162-170.
[14] Selini N., Elmeguenni M., Benguediab M. (2013) Effect of the Triaxiality in Plane Stress Conditions, *Eng. Technol. & Appl. Sci. Res.* **3**, 373–380.
[15] Kondori B., Benzerga A. A., Needleman A. (2018) Discrete shear-transformation-zone plasticity modeling of notched bars, *Journal of the Mechanics and Physics of Solids* **111**, 18–42.
[16] Zhai J., Luo T., Gao X., Graham S. M., Knudsen E. (2016) Modeling the ductile damage process in commercially pure titanium, *International Journal of Solids and Structures* **91**, 26-45.
[17] Lindner D., Mathieu F., Hild F., Allix O., Minh C.-H., Paulien-Camy O. (2015) On the evaluation of stress triaxiality fields in a notched titanium alloy sample via integrated digital image correlation, *Transactions of the ASME*, **82**, 071014, 1–10.
[18] Heibel S., Nester W., Clausmeyer T., Tekkayan A. E. (2017) Failure assessment in sheet metal forming using a phenomenological damage model and fracture criterion: experiments, parameter identification and validation, *Procedia Engineering*, **207**, 2066–2071.
[19] Orozco-Caballero A., Li F., Esqué-de los Ojos D., Atkinson M. D., Quinta da Fonseca J. (2018) On the ductility of alpha titanium: The effect of temperature and deformation mode, *Acta Materialia*, **149**, 1-10.
[20] Neilsen K.L., and Tvergaard V. (2010) Ductile shear failure or plug failure of spot welds modelled by modified Gurson model, *Eng. Fract. Mech.*, 77, 1031–1047.
[21] Tvergaard V. (2015) Study of localization in a void-sheet under stress states near pure shear, *International Journal of Solids and Structures*, **60–61**, 28–34.
[22] Zhai J., Luo T., Gao X., Graham S. M., Baral M., Korkolis Y. P., Knudsend E. (2016) Modeling the ductile damage process in commercially pure titanium, *International Journal of Solids and Structures*, **91**, 26–45.
[23] Corigliano A., Mariani S. and Orsatti B. (2000) Identification of Gurson–Tvergaard material model parameters via Kalman filtering technique. I. Theory, *International Journal of of Fracture*, 104, 349–373.
[24] Mirone G., Barbagallo R., Corallo D. (2016) A new yield criteria including the effect of lode angle and stress triaxiality, *Procedia Structural Integrity*, **2**, 3684–3696.
[24] Springmann M., Kuna M. (2005) Identification of material parameters of the Gurson–Tvergaard–Needleman model by combined experimental and numerical techniques, *Computational Materials Science*, 32, 544–552.
[25] Verleysen P. and Peirs J. (2017) Quasi-static and high strain rate fracture behaviour of Ti6Al4V, *International Journal of Impact Engineering*, **108**, 370-388.
[26] Zhang W., Cai Y. Continuum Damage Mechanics and Numerical Applications. *Springer Science & Business Media, 2010 - Technology & Engineering*, 1000 p.

[27] Zerilli F.J., Armstrong R.W. (1992) The effect of dislocation drag on the stress-strain behaviour of F.C.C. metals, *Acta Metall. Mater*, 40, 1803–1808.